New Anthracene-Containing Phenylene- or Thienylene-Vinylene Copolymers: Synthesis, Characterization, Photophysics, and Photovoltaics

Panagiotis D. Vellis,[1] John A. Mikroyannidis,[1] Diego Bagnis,[2] Luca Valentini,[2] Josè M. Kenny[2]

[1]*Chemical Technology Laboratory, Department of Chemistry, University of Patras, GR-26500 Patras, Greece*
[2]*Civil and Enviromental Engineering Department, NIPLAB-INSTM, University of Perugia, 05100 Terni, Italy*

Received 14 October 2008; accepted 23 December 2008
DOI 10.1002/app.29967
Published online 2 April 2009 in Wiley InterScience (www.interscience.wiley.com).

ABSTRACT: Four new conjugated alternating vinylene-copolymers, **PAP6**, **PAT**, **PA**, and **TAT**, incorporating anthracene rings along the backbone were synthesized by Heck coupling. They were very soluble in common organic solvents and absorbed at the range of 300–500 nm with optical band gaps of 2.38–2.47 eV. They behaved in solution as green emitters, with maximum photoluminescence at 455–518 nm. Finally, these soluble copolymers were used as donor material to realize bulk heterojunction solar cell with (6,6)-C_{61}-butyric acid methyl ester as the acceptor. More efficient photovoltaic cells were obtained from the copolymer that carried hexyloxy than dodecyloxy side groups. © 2009 Wiley Periodicals, Inc. J Appl Polym Sci 113: 1173–1181, 2009

Key words: synthesis; photophysics; phenylenevinylene; thienylenevinylene; anthracene; photovoltaic cells

INTRODUCTION

Over the last few decades, photovoltaic (PV) cells based on organic semiconducting materials have been actively investigated for low-cost alternatives to conventional inorganic PV cells. Conjugated polymers, especially, have tremendous potential for future PV cells because they can be easily processed and tailored to all needs due to the infinite variability of organic materials.

Organic soluble narrow band gap polymers are particularly desirable for photovoltaics due to their spectral absorption, which matches the solar terrestrial radiation.[1–4] They are also needed for deep red and near-infrared (IR) emitting devices,[1] for applications using *n*- and *p*-type conductors,[5] especially due to their potentially multicolored states.[6,7] The donor–acceptor approach (D–A) is one of the most effective ways of building a narrow band gap polymer. The high-lying HOMO of a donor fragment combined with the low-lying LUMO of an acceptor gives rise to a $-(D-A)_x-$ repeat unit structure with an unusually small HOMO-LUMO separation and narrow band gap.[8–10]

The presence of a double bond of a defined configuration (1) reduces the overall aromatic character of the planar structures and hence increases the *p*-electron localization, and (2) restricts the rotational freedom inherent to thiophenes,[11,12] which increases the energy-band gap.[13] The introduction of a vinylene unit into polymeric structures is a well-known method for forming coplanar molecules with an extended *p*-conjugated length, which should help to maximize the organization of the molecules in thin films.[14–16]

Anthracene is an organic semiconductor,[17–20] extensively investigated over many decades, and it consists of three linear phenyl rings in its crystal structure. The electronic conduction of anthracene is due to free electrons and holes present in the crystal. The activation energy of anthracene reported in the literature ranges from 0.9 to 1.6 eV based on the type of the sample and the technique involved.[21–28] Conductivity in anthracene is by two mechanisms, namely, by hopping (production of charge carriers) and/or by tunneling (mobility of charge carriers).

Mixing two polymers typically leads to phase separation and creation of microstructured D–A junctions. Additionally, with the use of D–A polymers of different band gaps, the device can be made sensitive over a wide spectral range. A η_P value of 1% and incident-photon-to-current conversion efficiency of 6% at low light intensities have been reported for a bulk-heterojunction system formed from two different conjugated polymers: poly[2-methoxy-5-(2-ethylhexyloxy)-1,4-phenylene vinylene] as the donor, in composite with cyano (CN) poly-dialkoxy-*p*-phenylenevinylene (PPV) as the acceptor.[29] Initially, solar cells made with blends of PPV derivatives have

Correspondence to: J. A. Mikroyannidis (mikroyan@chemistry.upatras.gr) and L. Valentini (mic@unipg.it).

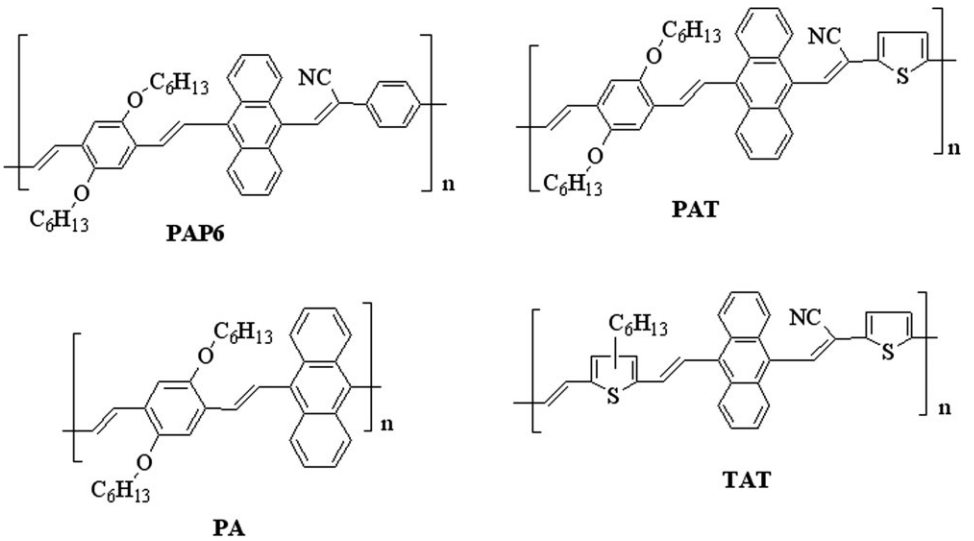

Chart 1 Chemical structure of copolymers PAP6, PAT, PA, and TAT.

given efficiencies lower than 1%.[30,31] In recent studies of blends of PPV-based donors together with a CN substituted PPV[32] or a red emitting polyfluorene[33] as acceptor, efficiencies exceeding 1.5% have been reported, thus approaching the efficiency of their fullerene counterparts.[34] A literature survey revealed that other anthracene-containing polymers have been used for PV devices reaching efficiencies up to 1.12%.[35]

CN groups could be used as the electron-withdrawing units. Materials with high electron affinities played a crucial role in the development of high-performance conjugated polymer optoelectronic devices.[36] The introduction of CN groups onto a poly(*p*-phenylenevinylene) backbone has been proved an effective way of lowering the LUMO level of the polymer.[30,37]

The present investigation describes the synthesis and characterization as well as the photophysical and photovoltaic properties of four new conjugated alternating anthracene-containing copolymers. They were successfully synthesized by Ziegler and Heck[38] coupling and contained solubilizing hexyl or hexyloxy side groups. The structures of these copolymers (**PAP6**, **PAT**, **PA**, and **TAT**) are shown in Chart 1. The names of the copolymers indicate their chemical structures and contain **P** for phenylene, **A** for anthracene, and **T** for thiophene. Three of the copolymers (**PAP6**, **PAT**, and **PA**) are *p*-phenylenevinylene derivatives, while one of them (**TAT**) is thienylenevinylene derivative. Copolymers **PAP6**, **PAT**, and **TAT** carried an additional CN-substituted olefinic bond.

The copolymers **PAP6**, **PAT**, and **TAT** had the architecture of D–A. Specifically, **PAP6** and **PAT** had the first moiety of *p*-dihexyloxyphenylene as donor and the second moiety with the anthracene and the CN vinylene bond as acceptor. Similarly, copolymer **TAT** had the first moiety of 3-hexylthiophene as donor and the same second moiety as acceptor. It has been well established that by alternating copolymerization of D and A the band gap of the resulting copolymer is narrowed.[8–10]

MATERIALS AND METHODS

Characterization methods

IR spectra were recorded on a Perkin–Elmer 16PC FTIR spectrometer with KBr pellets. ^{1}H-NMR (400 MHz) and ^{13}C-NMR (100 MHz) spectra were obtained by using a Bruker spectrometer. Chemical shifts (δ-values) are given in parts per million with tetramethylsilane as an internal standard. UV–vis spectra were recorded on a Beckman DU-640 spectrometer with spectrograde tetrahydrofuran (THF). The PL spectra were obtained with a Perkin–Elmer LS45 luminescence spectrometer. The PL spectra were recorded with the corresponding excitation maximum (400 nm) as the excitation wavelength.

Reagents and solvents

N,N-Dimethylformamide (DMF) and THF were dried by distillation over CaH_2. Triethylamine was purified by distillation over KOH. 2-(5-Bromothiophen-2-yl)acetonitrile was synthesized by bromination of thiophene-2-acetonitrile by means of *N*-bromosuccinimide in DMF.[39] All other reagents and solvents were commercially purchased and used as supplied.

Preparation of monomers

9-Bromoanthracene-10-carbaldehyde (1)

Bromine (0.39 g, 2.42 mmol) diluted with CH_2Cl_2 was added dropwise at room temperature to a stirred solution of 9-anthracaldehyde (0.50 g, 2.42 mmol) in CH_2Cl_2 (15 mL). The mixture was refluxed for 4 h and then was cooled at 4°C. Compound **1** precipitated as a yellow-green solid. A yellow purified sample was obtained by recrystallization from ethanol (0.60 g, yield 77%, mp 202–204°C).

FTIR (KBr cm^{-1}): 726, 758, 898, 1680.

^{1}H-NMR ($CDCl_3$, ppm): 11.40 (s, 1H, CHO); 8.88–7.93 (m, 4H, aromatic of anthracene at position 1, 4, 5, 8); 7.60–7.45 (m, 4H, aromatic of anthracene at position 2, 3, 6, 7).

Elem. Anal. for $C_{15}H_9BrO$: C, 63.18; H, 3.18. Found: C, 62.78; H, 3.12.

3-(9-Bromoanthracene-10-yl)-2-(4-bromophenyl) acrylonitrile (2)

A flask was charged with a solution of **1** (0.08 g, 0.28 mmol) and 4-bromophenylacetonitrile (0.05 g, 0.28 mmol) in anhydrous ethanol. A hot solution of NaOH (0.01 g, 0.32 mmol) in anhydrous ethanol was added dropwise under N_2. Stirring of the mixture was continued at room temperature for 5 h. The yellow precipitate was filtered, washed with water, and recrystallized from acetonitrile (0.09 g, yield, 69%; mp, 182–185°C).

FTIR (KBr, cm^{-1}): 736, 754, 904, 1440, 1618, 2224.

^{1}H-NMR ($CDCl_3$, ppm): [Fig. 1(a)] 8.59–8.56 (m, 4H, aromatic "a"); 7.97 (m, 1H, olefinic "c"); 7.67–7.65 (m, 4H, aromatic "b"); 7.63–7.65 (m, 4H, aromatic "d").

^{13}C-NMR ($CDCl_3$, ppm): [Fig. 1(b)] 140 (carbon "6"); 133 (carbon "5"); 132 (carbon "9"); 131 (carbon "10"); 130 (carbon "2"); 129 (carbon "3"); 128 (carbon "4"); 127 (carbon "11"); 125 (carbon "1"); 124 (carbon "8"); 99 (carbon "7").

Elem. Anal. for $C_{23}H_{13}Br_2N$: C, 59.64; H, 2.83; N, 3.02. Found: C, 58.72; H, 2.77; N, 3.00.

3-(9-Bromoanthracene-10-yl)-2-(5-bromothiophen-2-yl)acrylonitrile (3)

Compound **3** was similarly prepared as a green solid from the reaction of **1** with 2-(-5-bromothiophen-2-yl)acetonitrile. It was recrystallized from acetonitrile (0.123 g, 74%).

FTIR (KBr, cm^{-1}): 748, 758, 880, 1080, 1020, 1256, 1438, 1624, 2228, 2997.

^{1}H-NMR ($CDCl_3$, ppm): 8.43–8.45 (m, 4H, aromatic of anthracene at positions 1, 4, 5, 8); 7.69–7.74 (m, 4H, aromatic of anthracene at positions 2, 3, 6, 7); 7.60 (s, 1H, olefinic); 6.91 (m, 2H, aromatic of thiophene ring).

Elem. Anal. for $C_{21}H_{11}Br_2NS$: C, 53.76; H, 2.36; N, 2.99. Found: C, 52.86; H, 2.25; N, 2.93.

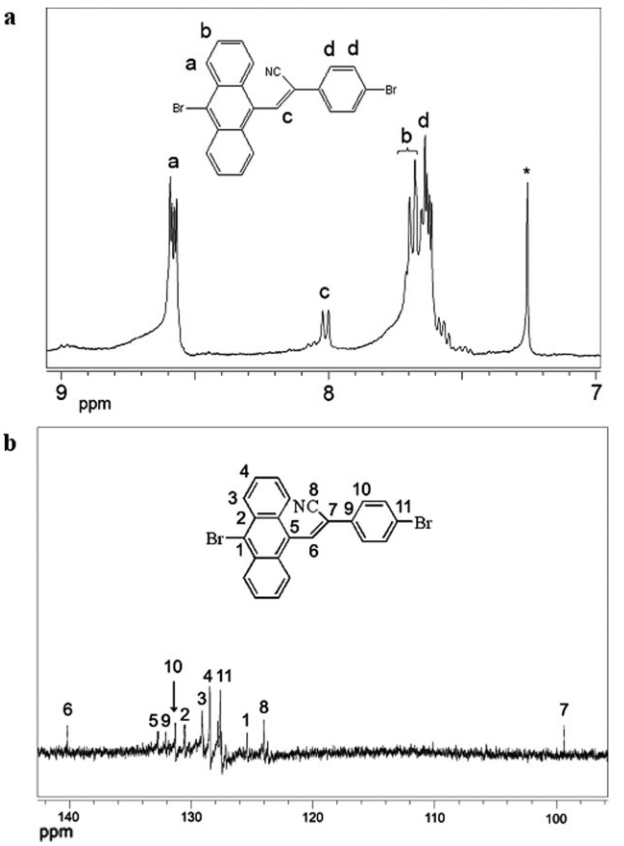

Figure 1 ^{1}H-NMR (a) and ^{13}C-NMR (b) spectra of dibromide **2** in $CDCl_3$ solution. The peak of the solvent in the ^{1}H-NMR spectrum is denoted with an asterisk.

2,5-Dihexyloxy-1,4-divinylbenzene (4)

The Stille coupling reaction[40] was used to prepare compound **4**. In particular, this compound was prepared by reacting 2,5-dihexyloxy-1,4-dibromobenzene with tributylvinyltin in the presence of the catalyst $PdCl_2(PPh_3)_2$ plus a few crystals of 2,6-di-*tert*-butylphenol, using toluene as a solvent.[41]

9,10-Dibromoanthracene (5)

Compound **5** was prepared according to a reported method.[42]

3-Hexyl-2,5-divinylthiophene (6)

This compound was prepared by Stille coupling reaction[40] of 2,5-dibromo-3-hexylthiophene with vinyltrimethylsilane.[43] The spectroscopic characterization of **6** conforms to literature.[43]

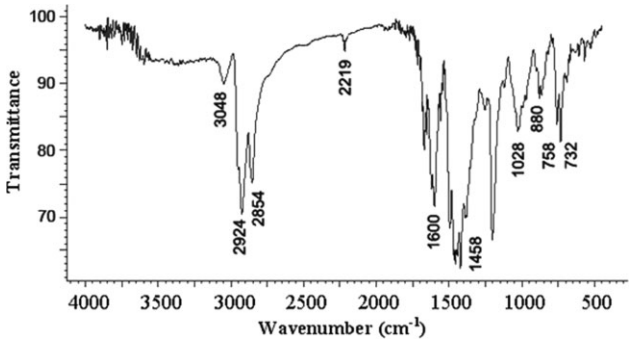

Figure 2 FTIR spectrum of copolymer **PAP6**.

Preparation of copolymers

The preparation of **PAP6** is given as a typical example from the preparation of copolymers. A flask was charged with a mixture of **4** (0.0960 g, 0.290 mmol), **2** (0.1345 g, 0.290 mmol), $Pd(OAc)_2$ (0.0027 g, 0.012 mmol), P(*o*-tolyl)$_3$ (0.0200 g, 0.066 mmol), DMF (8 mL), and triethylamine (2 mL). The flask was degassed and purged with N_2. The mixture was heated at 90°C for 24 h under N_2. Then, it was filtered and the filtrate was poured into methanol. The yellow precipitate was filtered and washed with methanol. The crude product was purified by dissolving in THF and precipitating into methanol (0.12 g, 65%).

FTIR (KBr, cm^{-1}): (Fig. 2) 732, 758, 880, 898, 1028, 1202, 1420, 1458, 1600, 1618, 2219, 2854, 2924, 3048.

^{1}H-NMR ($CDCl_3$, ppm): (Fig. 3) 8.32 (m, 4H, aromatic "g"); 7.82 (s, 1H, olefinic "i"); 7.50 (m, 4H, aromatic "h"); 7.43 (m, 4H, aromatic "j"); 7.07 (m, 4H, olefinic "f"); 6.90 (m, 2H, aromatic "e"); 4.01 (m, 4H, aliphatic "d"); 1.87 (m, 4H, aliphatic "c"); 1.25 (m, 12H, aliphatic "b"); 0.90 (m, 6H, aliphatic "a").

Elem. Anal. for $(C_{45}H_{45}NO_2)_n$: C, 85.54; H, 7.18; N, 2.22. Found: C, 84.38; H, 7.07; N, 2.19.

Copolymer **PAT** was similarly prepared in 78% yield from the reaction of **4** with **3**.

FTIR (KBr, cm^{-1}): 734, 758, 898, 980, 1030, 1202, 1420, 1458, 1618, 2219, 2854, 2926, 3046.

^{1}H-NMR ($CDCl_3$, ppm): 8.48 (m, 4H, aromatic of anthracene at positions 1, 4, 5, 8); 8.03 (m, 4H, aromatic of anthracene at positions 2, 3, 6, 7); 7.95 (s, 1H, olefinic of the CN vinylene); 6.99 (m, 2H, aromatic of phenyl ring); 6.96 (m, 4H, olefinic); 6.92 (m, 2H, aromatic of thiophene ring); 4.05 (m, 4H, OCH_2); 1.82 (m, 4H, OCH_2CH_2); 1.25 (m, 12H, $O(CH_2)_2(CH_2)_3$); 0.92 (m, 6H, $O(CH_2)_2(CH_2)_3CH_3$).

Elem. Anal. for $(C_{43}H_{43}NO_2S)_n$: C, 80.97; H, 6.79; N, 2.20. Found: C, 79.53; H, 6.71; N, 2.14.

Copolymer **PA** was prepared in 68% yield from the reaction of **4** with **5**.

FTIR (KBr, cm^{-1}): 754, 862, 994, 1028, 1204, 1468, 1622, 2860, 2928, 2954, 3050.

^{1}H-NMR ($CDCl_3$, ppm): 8.59 (m, 4H, aromatic of anthracene at positions 1, 4, 5, 8); 7.62 (m, 4H, aromatic of anthracene at positions 2, 3, 6, 7); 7.09 (m, 2H, aromatic of phenyl ring); 6.98 (m, 4H, olefinic); 3.94 (m, 4H, OCH_2); 1.80 (m, 4H, OCH_2CH_2); 1.28 (m, 12H, $O(CH_2)_2(CH_2)_3$); 0.98 (m, 6H, $O(CH_2)_2(CH_2)_3CH_3$).

Elem. Anal. for $(C_{36}H_{40}O_2)_n$: C, 85.67; H, 7.99. Found: C, 83.92; H, 7.84.

Copolymer **TAT** was prepared in 74% yield by reacting **6** with **3** by Heck[38] coupling reaction.

FTIR (KBr, cm^{-1}): 734, 754, 840, 882, 974, 1028, 1084, 1258, 1376, 1462, 1611, 2224, 2854, 2922, 2954, 3052.

^{1}H-NMR ($CDCl_3$, ppm): 8.59 (4H, aromatic of anthracene at positions 1, 4, 5, 8); 7.63 (m, 4H, aromatic of anthracene at positions 2, 3, 6, 7); 7.47 (s, 1H, olefinic of the CN vinylene); 6.94 (m, 3H, aromatic of thiophene rings); 7.02 (m, 4H, olefinic); 2.51 (m, 2H, $CH_2(CH_2)_4$); 1.28–1.31 (m, 8H, $CH_2(CH_2)_4$); 0.92 (m, 3H, $(CH_2)_5CH_3$).

Elem. Anal. for $(C_{35}H_{29}NS_2)_n$: C, 79.66; H, 5.54; N, 2.65. Found: C, 77.82; H, 5.45; N, 2.60.

Device fabrication

The solar cell was fabricated with the structure of indium tin-oxide (ITO)/poly(3,4-ethylenedioxythiophene (PEDOT): poly(styrenesulfonate) (PSS)/active layer/LiF/Al. The ITO glass was previously precleaned and plasma treated in oxygen atmosphere (5 min, 8.0×10^{-2} Torr, −300 V bias substrate) and modified by a thin layer of PEDOT : PSS (Baytron P®), which was spin-cast (4000 rpm) from a PEDOT : PSS aqueous solution on the plasma-treated ITO substrate and was dried subsequently at 150°C for

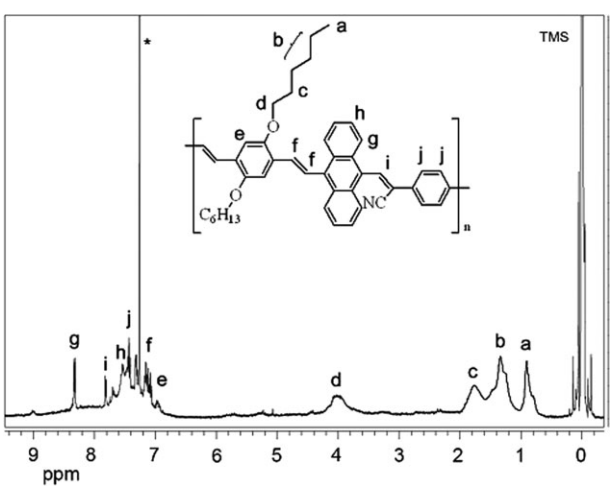

Figure 3 ^{1}H-NMR spectrum of copolymer **PAP6** in $CDCl_3$ solution. The peak of the solvent is denoted with an asterisk.

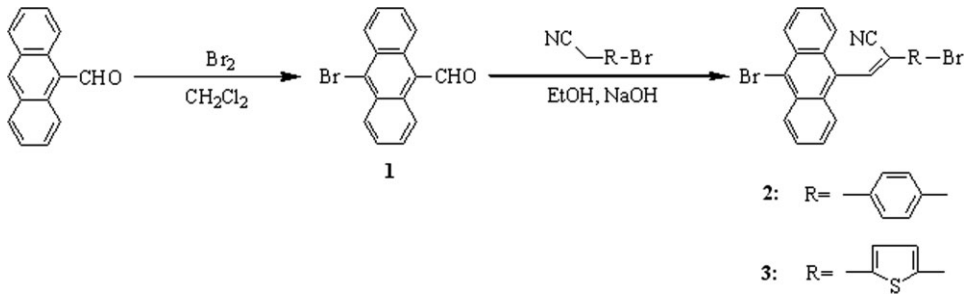

Scheme 1 Synthesis of the key dibromides **2** and **3**.

10 min in air. The thickness of the PEDOT : PSS layer was 30 nm. The photosensitive layer was prepared by spin-coating (2000 rpm) the $CHCl_3$ solution of the PAP12/PCBM, PAP6/PCBM, PAT/PCBM, PA/PCBM, and TAT/PCBM (1 : 3 weight ratio) blends with the solution concentration of 20 mg/mL on the ITO/PEDOT : PSS electrode. The thickness of the photosensitive layer was optimized to 150 nm by adjusting the rotating speed of the spin-coating and was measured with an atomic force microscopy. Then the top metal electrode, which is made up of LiF and Al, was deposited on the active layer by vacuum evaporation ($\approx 10^{-6}$ Torr) with an optimized thickness of 0.7 and 60 nm, respectively. Fifteen electrodes with an effective area of 3 mm^2 were deposited for each sample. The current–voltage (I–V) measurement of the devices was conducted on a computer-controlled Keithley 4200 Source Measure Unit. A halogen lamp was used as the white light source, and the optical power (P_{in}) of the sample was 44 mW/cm^2.

The power conversion efficiency (PCE) (η) of the photovoltaic cells was calculated by using the following equations:

$$\eta = FF \times V_{oc} \times J_{sc}/P_{in}$$

$$FF = V_{max} \times J_{max}/V_{oc} \times J$$

where P_{in} is the power of the incident light, V_{oc} is the open-circuit voltage, and J_{sc} is the short-circuit current density. V_{max} and J_{max} represent the voltage and current densities at maximum power. A Perkin–Elmer Lambda 35 UV spectrophotometer was used to monitor the absorption spectra of the films used to prepare the active layer.

RESULTS AND DISCUSSION

Synthesis and characterization

Scheme 1 outlines the preparation of the key-dibromides **2** and **3**. In particular, 10-bromo-9-anthracenecarboxaldehyde (**1**), which was synthesized by bromination of 9-anthracenecarboxaldehyde, reacted with 4-bromophenylacetonitrile or 2-(5-bromothiophen-2-yl)acetonitrile in anhydrous ethanol in the presence of NaOH to afford **2** and **3**, respectively. These dibromides were characterized by FTIR and ^{1}H-NMR spectroscopy.

Figure 1(a,b) depicts the ^{1}H-NMR and ^{13}C-NMR spectra of dibromide **2**. The ^{1}H-NMR spectrum displayed an upfield multiplet at 8.59–8.56 ppm assigned to the anthracene protons labeled "a." The other anthracene protons labeled "b" resonated at 7.67–7.65 ppm and they were partially overlapped with the phenylene protons labeled "d." The CN-vinylene proton labeled "c" gave a signal at 7.97 ppm. Usually, the vinylene protons appear at 6.90–7.00 ppm but the proton "c" showed higher shift due to the presence of the electron withdrawing CN group on the vinylene bond.

The ^{13}C-NMR spectrum of **2** [Fig. 1(b)] showed two distinguishable peaks at 140 and 99 ppm assigned to the two carbons, "6" and "7," respectively, of the CN-substituted vinylene bond. The carbon "8" of the CN group resonated at 124 ppm, while the other aromatic carbons resonated at the region of 127–133 ppm.

Three new *p*-phenylenevinylene alternating copolymers were prepared by Heck coupling reaction[38] according to Scheme 2. Specifically, **4** reacted with **2**, **3**, or **5** to afford the copolymers **PAP6**, **PAT**, and **PA**, respectively. In addition, the thienylenevinylene alternating copolymer **TAT** was similarly prepared by reacting **6** with **3** (Scheme 3). The polymerization reactions took place in DMF utilizing $Pd(OAc)_2$ and Et_3N as catalyst and proton scavenger, respectively. The copolymers were very soluble in common organic solvents (THF, dichloromethane, chloroform, toluene) owing to the hexyloxy or hexyl side groups. The preparation yields were 65–78%. The number-average molecular weights (M_n) of the copolymers were 12,800–9900 with a polydispersity of 1.9–1.5 (Table I).

The FTIR and ^{1}H-NMR spectra of the copolymers were consistent with their chemical structures. Figures 2 and 3 present the FTIR and ^{1}H-NMR spectra of **PAP6**. The IR spectrum showed characteristic absorption bands at 3048, 1600, 1458 (aromatic);

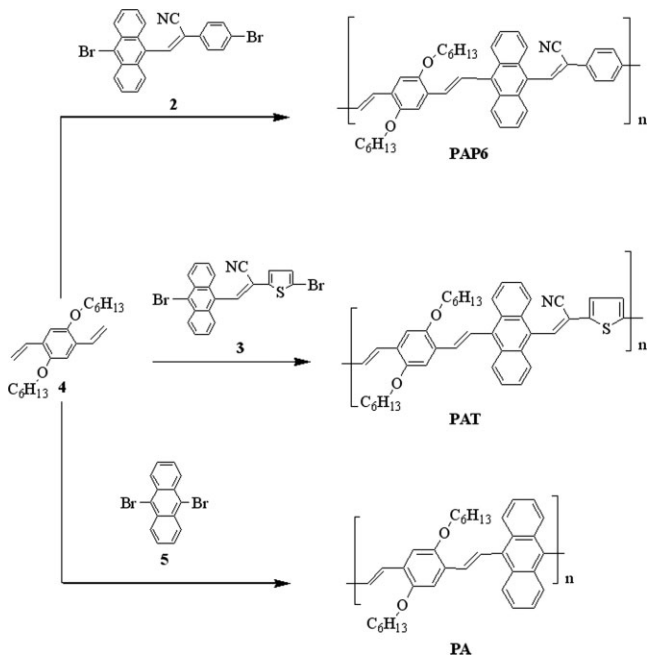

Scheme 2 Synthesis of copolymers **PAP6**, **PAT**, and **PA**.

2924, 2854 (C—H stretching of hexyloxy groups); 1202, 1028 (ether bond); 880, 758, 732 (anthracene ring); 970 (trans-olefinic bond) and 2219 cm^{-1} (CN group). **TAT** lacked of the absorptions associated with the ether bond. Figure 3 depicts the ^{1}H-NMR spectrum of **PAP6**. The aromatic protons labeled "g," "h," "j," and "e" resonated at 8.32, 7.50, 7.43, and 6.90 ppm, respectively. The aromatic protons "e" showed the most downfield resonance among the aromatic protons due to the shielding effect caused by the electron donating hexyloxy groups. The olefinic protons "i" and "f" appeared at 7.82 and 7.07 ppm, respectively. The aliphatic protons "a," "b," "c," and "d" gave peaks at 0.90, 1.25, 1.87, and 4.01 ppm, respectively. Finally, the small signal between 5 and 6 ppm are from the CH_2=CH— vinyl terminal groups.

Photophysical properties

The photophysical properties of the copolymers were investigated in both dilute THF solution

TABLE I
Preparation Yields and Molecular Weights of Copolymers

Copolymer	Preparation yields (%)	M_n[a]	M_w/M_n[a]
PAP6	65	12,800	1.9
PAT	78	9900	1.3
PA	68	11,200	1.6
TAT	74	10,500	1.5
PAP12	71	12,600	1.8

[a] Molecular weights determined by GPC using polystyrene standards.

($10^{-5}M$) and thin film and are summarized in Table II. The normalized UV–vis absorption spectra of the four copolymers in solution and in thin film are shown in Figure 4(a,b). The normalized PL emission spectra in solution are shown in Figure 5. Because the copolymers were not strongly photoluminescent in solid state, their PL emission spectra in thin film could not be obtained.

The absorption spectra of copolymers (Fig. 4) displayed a long-wave absorption at 400–430 nm, which was assigned to the π-π* transition of the conjugated backbone. The absorption of anthracene is located at the range of 300–390 nm.[44] Generally, the absorption spectra of these copolymers were broad and extended from about 300 to 500 nm, which is an attractive feature for their photovoltaic properties.

The optical band gaps (E_gs) of the copolymers, calculated from the onset of the absorption spectra in thin film, were almost the same (2.38–2.39 eV) for **PAP6**, **PAT**, and **TAT**, while **PA** had a slightly higher E_g of 2.47 eV (Table II).

Upon photoexcitation at the excitation maximum (400 nm), the solutions of the copolymers emitted green-yellow light with maximum ($\lambda_{f,max}$) at 455–518 nm (Fig. 5). **TAT** showed the most blue-shifted $\lambda_{f,max}$ among the four copolymers because it has one hexyl per repeating unit instead of the two hexyloxy groups. It has been well established that the hexyloxys were more efficient electron-donating groups than the hexyl groups.[45] **PAP6** and **PAT** displayed $\lambda_{f,max}$ at 502 and 518 nm, respectively, which is in line with their $\lambda_{a,max}$ in thin film (Table II). Thus, the replacement of the phenylene with the thienylene ring seems to favor π-electron delocalization along

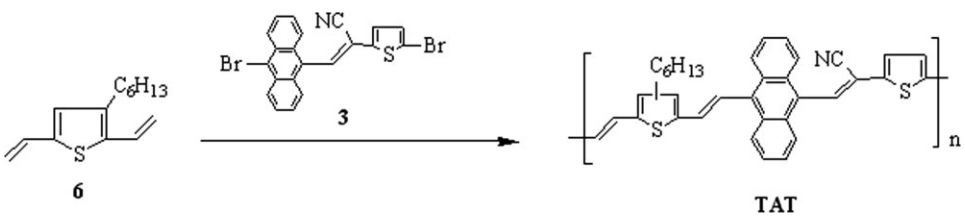

Scheme 3 Synthesis of copolymers **TAT**.

TABLE II
Photophysical Properties of Copolymers

Copolymer	$\lambda_{a,max}$[a] in solution (nm)	$\lambda_{f,max}$[b] in solution (nm)	$\lambda_{a,max}$[a] in thin film (nm)	E_g[c] (eV)
PAP6	390	502	403	2.38
PAT	403	518	433	2.39
PA	404	468 (495)[d]	409	2.47
TAT	390	455	395	2.38

The PL emission spectra were recorded by using the corresponding excitation maximum as excitation wavelength (400 nm).

[a] $\lambda_{a,max}$: The absorption maximum from the UV–vis spectra in THF solution ($10^{-5}M$) or in thin film.

[b] $\lambda_{f,max}$: The PL emission maximum in THF solution ($10^{-5}M$).

[c] E_g: The optical band gap calculated from the onset of thin film absorption spectrum.

[d] Value in bracket exhibits a shoulder in the emission spectra.

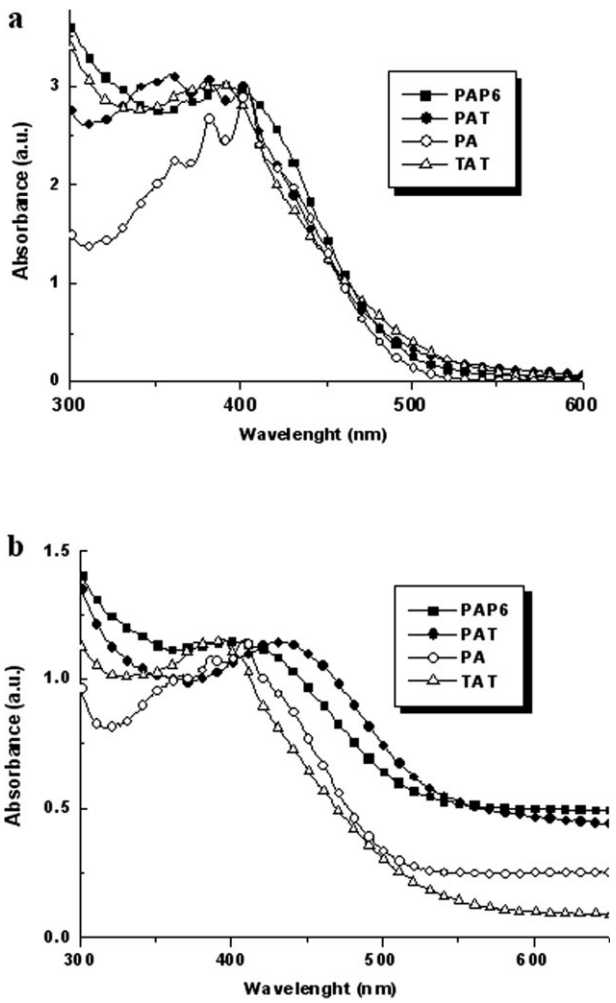

Figure 4 Normalized UV–vis absorption spectra of copolymers in THF solution ($10^{-5}M$) (a) and in thin films (b).

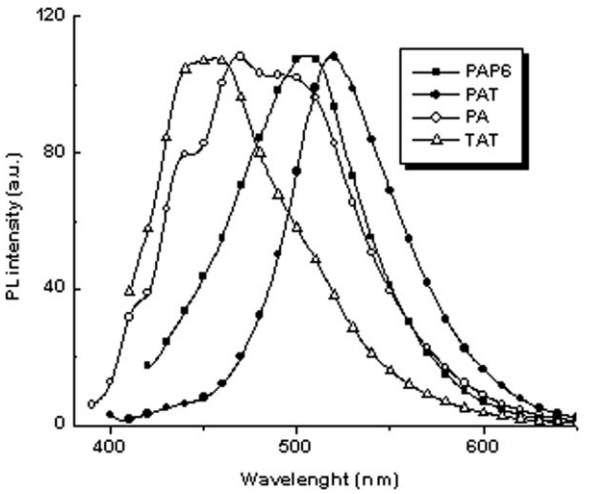

Figure 5 Normalized PL emission spectra of copolymers in THF solution ($10^{-5}M$). The PL emission spectra were recorded by using the excitation maximum (400 nm) as excitation wavelength.

the backbone. **PA** showed absolute $\lambda_{f,max}$ at 468 nm and a shoulder at 495 nm, which are blue-shifted relative to **PAP6** and **PAT**. This behavior could be attributed to the absence of the CN-substituted olefinic bond.

Photovoltaic properties

Copolymer **PAP12** (Chart 2), which has the same chemical structure with that of **PAP6** but carries dodecyloxy instead of hexyloxy side groups, was synthesized for comparative purposes. In particular, the effect of the length of the alcoxy side groups of these copolymers (**PAP6** and **PAP12**) on the compatibility with PCBM and subsequently on the device efficiency was investigated. Copolymer **PAP12** was synthesized in 71% yield by reacting 2,5-didodecyloxy-1,4-divinylbenzene with **2**. It had M_n of 12,600, M_w/M_n of 1.8 (Table I), and its spectroscopic data were in line with those of **PAP6**.

Figure 6 depicts the absorption spectra the copolymer/PCBM films (1 : 3 weight ratio), which was prepared by spin-coating from $CHCl_3$. The peak at 333 nm in the absorption spectrum of the **PAP12**/PCBM film is due to the absorption peak of PCBM. This

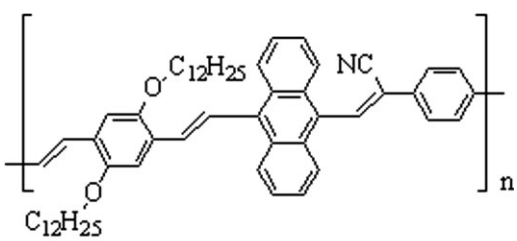

PAP12

Chart 2 Chemical structure of copolymer **PAP12**.

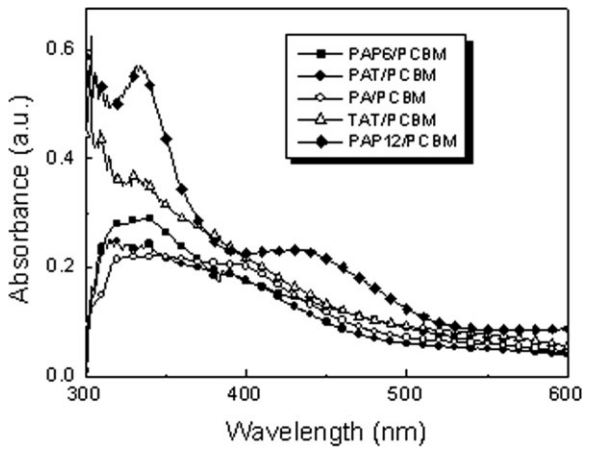

Figure 6 UV–vis spectra of **PAP12**/PCBM, **PAP6**/PCBM, **PAT**/PCBM, **PA**/PCBM, and **TAT**/PCBM films (1 : 3 weight ratio).

feature is less evident in the other copolymer/PCBM films, being this effect most probably is due to a better dispersion and hence a better compatibilization of the PCBM with the shorter alkyl chains. This reasoning has been confirmed by atomic force microscopy analysis (images not shown). It has been found

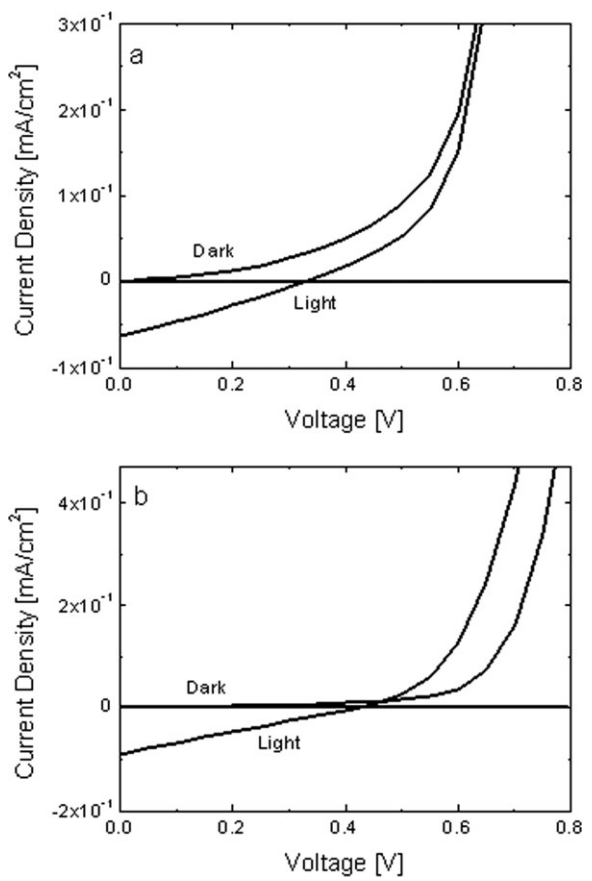

Figure 7 Current density–voltage curves in the dark and under illumination of the polymeric solar cells based on **PAP12**/PCBM (a) and **PAP6**/PCBM (b).

TABLE III
Solar Cell Characteristics of Copolymers PAP12 and PAP6

Copolymer	V_{oc}[a] (mV)	J_{sc}[b] (mA/cm^2)	FF[c]	PCE[d]
PAP12	0.32	0.063	0.29	0.013
PAP6	0.41	0.090	0.25	0.021

[a] V_{oc}: open-circuit voltage.
[b] J_{sc}: short-circuit current density.
[c] FF: fill factor.
[d] PCE: power conversion efficiency.

that the surface topography of the film from the **PAP12**/PCBM blend is significantly rougher [root mean square roughness (rms) of 5.2 nm] than the film from the **PAP6**/PCBM blend (rms of 1.5 nm).

An examination of the solar cell characteristics reported in Figure 7 and summarized in Table III indicates that the copolymer chemical architecture influences the photovoltaic behavior. In particular, photovoltaic behavior was recorded only for the **PAP12** and **PAP6** copolymers. The comparison of the solar cell characteristics shows an increase of the open-circuit voltage (V_{oc}) and the short-circuit current density (J_{sc}) for the **PAP6**/PCBM blend with respect to the **PAP12**/PCBM blend. This indicates that the length of the alcoxy side groups affects the characteristics of the PV cells. In general it is known that the V_{oc} changes are due to the energy level of the donor and acceptor[46] and a combined study of the optical properties with the electrochemical characteristics to understand how the HOMO and LUMO levels are changing by changing the chemical tailoring is needed. This point is currently under investigation.

From the data reported in Table III, it was pointed out that the PCE of these systems are generally modest. This could possibly be attributed to the low overlap of the absorption of the donor material (**PAP6** or **PAP12**) with solar emission spectrum, so that resulting short circuit current density is not high. Moreover, the optical properties and photovoltaic performance of the cell are also affected by the film morphology and phase separation of the blend. These preliminary PV results were obtained without optimization of the solvent utilized for the preparation of the films, film thickness, and post annealing of the devices.

CONCLUSIONS

We synthesized by Heck coupling reaction new *p*-phenylenevinylene alternating copolymers (**PAP6**, **PAT**, and **PA**) and thienylenevinylene alternating copolymer (**TAT**) with anthracene rings along the backbone. They carried hexyl or hexyloxy side groups, which enhanced the solubility. The

absorption curves were broad and located approximately from 300 to 500 nm with optical band gaps of 2.38–2.47 eV. The solutions of the copolymers emitted green-yellow light with a maximum at 455–518 nm. Finally, it was reported how in perspective the high solubility of these copolymers in common organic solvents allows the preparation of bulk heterojunction photovoltaic devices. The device made from **PAP6** gave better characteristics than that made from **PAP12**.

References

1. Yang, R.; Tian, R.; Yan, J.; Zhang, Y.; Yang, J.; Hou, Q.; Yang, W.; Zhang, C.; Cao, Y. Macromolecules 2005, 38, 244.
2. Zhang, F.; Perzon, E.; Wang, X.; Mammo, W.; Andersson, M. R.; Inganas, O. Adv Funct Mater 2005, 15, 745.
3. Xia, Y.; Luo, J.; Deng, X.; Li, X.; Li, D.; Zhu, X.; Yang, W.; Cao, Y. Macromol Chem Phys 2006, 207, 511.
4. Wienk, M. M.; Turbiez, M. G. R.; Struijk, M. P.; Fonrodona, M.; Janssen, R. A. J Appl Phys Lett 2006, 88, 153511.
5. Arbizzani, C.; Catellani, M.; Mastragostino, M.; Mingazzini, C. Electrochim Acta 1995, 40, 1871.
6. Arbizzani, C.; Cerroni, M. G.; Mastragostino, M. Sol Energy Mater Sol Cells 1999, 56, 205.
7. Du Bois, C. J. Jr.; Larmat, F.; Irvin, D. J.; Reynolds, J. R. Synth Met 2001, 119, 321.
8. Thomas, C. A.; Zong, K.; Abboud, K. A.; Steel, P. J.; Reynolds, J. R. J Am Chem Soc 2004, 126, 16440.
9. Van Mullekom, H. A. M.; Vekemans, J. A. J. M.; Havinga, E. E.; Meijer, E. W. Mater Sci Eng 2001, 32, 1.
10. Wienk, M. J.; Struijk, P.; Janssen, R. A. J Chem Phys Lett 2006, 422, 488.
11. Distefano, G.; Da Colle, M.; Jones, D.; Zambianchi, M.; Favvafetto, L.; Modelli, A. J Phys Chem 1993, 97, 3504.
12. Orti, E.; Viruela, P. M.; Sanchez-Marin, J.; Tomas, F. J Phys Chem 1995, 99, 4955.
13. Roncali, J. Chem Rev 1997, 97, 173.
14. Hou, J.; Tan, Z.; Yan, Y.; He, Y.; Yang, C.; Li, Y. J Am Chem Soc 2006, 128, 4911.
15. Hou, J.; Huo, L.; He, C.; Yang, C.; Li, Y. Macromolecules 2006, 39, 594.
16. Zou, Y.; Wu, W.; Sang, G.; Yang, Y.; Liu, Y.; Li, Y. Macromolecules 2007, 40, 7231.
17. Bree, A.; Carswell, D. J.; Lyons, L. E. J Chem Soc 1955,1728.
18. Lyons, L. E.; Morris, G. C. J Chem Soc 1957,3648.
19. Choi, S.; Rice, S. A. J Chem Phys 1963, 38, 366.
20. Weisz, S. Z.; Jarnagin, R. C.; Silver, M. J Chem Phys 1964, 40, 3365.
21. Eley, D. D.; Parfitt, G. D.; Perry, M. J.; Taysum, D. H. Trans Faraday Soc 1953, 49, 79.
22. Mette, H.; Pick, H. Z Phys 1953, 134, 566.
23. Inokuchi, H. Bull Chem Soc Jpn 1956, 29, 131.
24. Northrop, D. C.; Simpson, O. Proc R Soc A 1956, 234, 124.
25. Kommandeur, J.; Schneider, W. G. J Chem Phys 1958, 28, 582.
26. LeBlanc, O. H. J Chem Phys 1961, 35, 1275.
27. Kokado, H.; Schneider, W. G. J Chem Phys 1964, 40, 2937.
28. Joseph, J. V.; Xavier, F. P. Bull Mater Sci 1997, 21, 1.
29. Yu, G.; Heeger, A. J. J Appl Phys 1995, 78, 4510.
30. Halls, J. J. M.; Walsh, C. A.; Greenham, N. C.; Marseglia, E. A.; Friend, R. H.; Moratti, S. C.; Holmes, A. B. Nature 1995, 376, 498.
31. Veenstra, S. C.; Verhees, W. J. H.; Kroon, J. M.; Koetse, M. M.; Sweelssen, J.; Bastiaansen, J. J. A. M.; Schoo, H. F. M.; Yang, X.; Alexeev, A.; Loos, J.; Schubert, U. S.; Wienk, M. M. Chem Mater 2004, 16, 2503.
32. Kietzke, T.; Hörhold, H.-H.; Neher, D. Chem Mater 2005, 17, 6532.
33. Koetse, M. M.; Sweelssen, J.; Hoekerd, K. T.; Schoo, H. F. M.; Veenstra, S. C.; Kroon, J. M.; Yang, X.; Loos, J. Appl Phys Lett 2006, 88, 083504.
34. Shaheen, S. E.; Brabec, C. J.; Sariciftci, N. S.; Padinger, F.; Fromherz, T.; Hummelen, J. C. Appl Phys Lett 2001, 78, 841.
35. Valentini, L.; Bagnis, D.; Marrocchi, A.; Seri, M.; Taticchi, A.; Kenny, J. M. Chem Mater 2008, 20, 32.
36. Hide, F.; Greenwald, Y.; Wudl, F.; Heeger, A. J. Synth Met 1997, 85, 1255.
37. Zou, Y.; Hou, J.; Yang, C.; Li, Y. Macromolecules 2006, 39, 8889.
38. Ziegler, C. B. Jr.,Heck, R. F. Org Chem 1978, 43, 2941.
39. Lee, J.; Cho, N. S.; Lee, S.; Shim, H.-K. Synth Met 2005, 155, 73.
40. McKean, D. R.; Parrinello, G.; Renaldo, A. F.; Stille, J. K. J Org Chem 1987, 52, 422.
41. Peng, Q.; Li, M.; Tang, X.; Lu, S.; Peng, J.; Cao, Y. J Polym Sci Part A: Polym Chem 2007, 45, 1632.
42. Cakmak, O.; Ramazan, E.; Tutar, A.; Celik, N. J Org Chem 2006, 71, 1795.
43. Adkins, C. T.; Harth, E. Macromolecules 2008, 41, 3472.
44. Selvaraj, S. L.; Xavier, F. P. J Cryst Growth 2001, 233, 583.
45. He, J.; Su, Z.; Yan, B.; Xiang, L.; Wang, Y. J Macromol Sci Pure Appl Chem 2007, 44, 989.
46. Brabec, C. J.; Cravino, A.; Meissner, D.; Sariciftci, N. S.; Fromherz, T.; Rispens, M. T.; Sanchez, L.; Hummelen, J. C. Adv Funct Mater 2001, 11, 374.